available at www.sciencedirect.com
journal homepage: www.europeanurology.com

European Association of Urology

Platinum Priority – Bladder Cancer – Editor's choice

Editorial by Jason R. Brown, Guru P. Sonpavde, Adam Calaway, Pedro C. Barata on pp. 312–314 of this issue

Whole-genome Mutational Analysis for Tumor-informed Detection of Circulating Tumor DNA in Patients with Urothelial Carcinoma

Iver Nordentoft [a,,†], Sia Viborg Lindskrog [a,b,†], Karin Birkenkamp-Demtröder [a,b], Santiago Gonzalez [c], Maja Kuzman [c], Jurica Levatic [c], Dunja Glavas [c], Ryan Ptashkin [c], James Smadbeck [c], Danielle Afterman [d], Tomer Lauterman [d], Yarin Cohen [d], Zohar Donenhirsh [d], Iman Tavassoly [c], Ury Alon [d], Amanda Frydendahl [a,b], Mads Heilskov Rasmussen [a,b], Claus Lindbjerg Andersen [a,b], Philippe Lamy [a], Michael Knudsen [a], Paz Polak [c], Asaf Zviran [c], Boris Oklander [d], Mads Agerbæk [e], Jørgen Bjerggaard Jensen [b,f], Lars Dyrskjøt [a,b,*]*

[a] *Department of Molecular Medicine, Aarhus University Hospital, Aarhus, Denmark;* [b] *Department of Clinical Medicine, Aarhus University, Aarhus, Denmark;* [c] *C2i Genomics, New York, NY, USA;* [d] *C2i Genomics, Haifa, Israel;* [e] *Department of Oncology, Aarhus University Hospital, Aarhus, Denmark;* [f] *Department of Urology, Aarhus University Hospital, Aarhus, Denmark*

Article info

Article history:
Accepted May 16, 2024

Associate Editor:
Laura Bukavina

Keywords:
Bladder cancer
Muscle-invasive bladder cancer
Urothelial carcinoma
Circulating tumor DNA
Liquid biopsies
Whole-genome sequencing
Tumor evolution

Abstract

Background and objective: Circulating tumor DNA (ctDNA) can be used for sensitive detection of minimal residual disease (MRD). However, the probability of detecting ctDNA in settings of low tumor burden is limited by the number of mutations analyzed and the plasma volume available. We used a whole-genome sequencing (WGS) approach for ctDNA detection in patients with urothelial carcinoma.
Methods: We used a tumor-informed WGS approach for ctDNA-based detection of MRD and evaluation of treatment responses. We analyzed 916 longitudinally collected plasma samples from 112 patients with localized muscle-invasive bladder cancer who received neoadjuvant chemotherapy (NAC) before radical cystectomy. Recurrence-free survival (primary endpoint), overall survival, and ctDNA dynamics during NAC were assessed.
Key findings and limitations: We found that WGS-based ctDNA detection is prognostic for patient outcomes with a median lead time of 131 d over radiographic imaging. WGS-based ctDNA assessment after radical cystectomy identified recurrence with sensitivity of 91% and specificity of 92%. In addition, genomic characterization of post-treatment plasma samples with a high ctDNA level revealed acquisition of platinum therapy–associated mutational signatures and copy number variations not present in the primary tumors. The sequencing depth is a limitation for studying tumor evolution.
Conclusions and clinical implications: Our results support the use of WGS for ultrasensitive ctDNA detection and highlight the possibility of plasma-based tracking of tumor evolution. WGS-based ctDNA detection represents a promising option for clinical use

† These authors contributed equally to this work.
* Corresponding authors. Department of Molecular Medicine, Aarhus University Hospital, Palle Juul-Jensens Boulevard 99, 8200 Aarhus N, Denmark.
E-mail addresses: iver.nordentoft@clin.au.dk (I. Nordentoft) lars@clin.au.dk (L. Dyrskjøt).

https://doi.org/10.1016/j.eururo.2024.05.014

owing to the low volume of plasma needed and the ease of performing WGS, eliminating the need for personalized assay design.

ADVANCING PRACTICE

What does this study add?

Our study supports the clinical potential of using a tumor-informed WGS-based strategy for sensitive ctDNA detection in patients with MIBC. WGS-based ctDNA detection has low requirements for plasma input and facilitates local sample processing without any need for designing bespoke assays for each patient, while still allowing patient customization through computational modeling. Thus, WGS-based ctDNA detection constitutes a promising option for clinical implementation of ctDNA testing.

Clinical Relevance

The article demonstrates that, in addition to further validating the role of ctDNA as a prognostic factor in urothelial cancer, the use of WGS-based ctDNA assessment enables the potential tracking of tumor evolution as patients progress through treatment paradigms. This approach allows for both the monitoring of disease recurrence and the detection of tumor evolution, facilitating rapid and precision-based treatment interventions before conventional radiographic imaging can provide evidence of recurrence.

Associate Editor Laura Bukavina, M.D., MPH

Patient Summary

Detection of tumor DNA in blood samples from patients with cancer of the urinary tract is associated with poorer outcomes. Disease recurrence after surgery can be identified by the presence of tumor DNA in blood before it can be detected on radiography scans.

1. Introduction

Recent studies have shown that circulating tumor DNA (ctDNA) is a powerful biomarker for early detection of recurrence and monitoring of treatment responses in multiple cancer types [1,2] including bladder cancer [3–6]. Curative-intent radical cystectomy (RC) preceded by neoadjuvant chemotherapy (NAC) is a standard of care for localized muscle-invasive bladder cancer (MIBC). However, nearly half of patients will experience recurrence, mainly within the first 2 yr after surgery [7]. Therefore, reliable diagnostic and prognostic biomarkers are needed for better detection of minimal residual disease (MRD) and recurrence to guide adjuvant treatment and to prompt oncological treatment of recurrence at an early time point. With the low tumor fractions typically observed after surgery, the probability of detecting ctDNA is limited by the number of mutations analyzed, the plasma volume available, and the sequencing depth [8]. Recent studies have demonstrated the feasibility of using tumor-informed whole-genome sequencing (WGS) for ultrasensitive ctDNA detection [9,10]. Here, we used a tumor-informed WGS-based approach for ctDNA detection in 112 patients with MIBC. Furthermore, we performed a *de novo* genomic characterization of plasma samples with a high ctDNA level to explore the potential for characterizing tumor evolution.

2. Patients and methods

The Supplementary material provides full details of the clinical samples and the methods used.

2.1. Patients and biological samples

In total, 112 patients diagnosed with MIBC treated with NAC and RC were enrolled between 2013 and 2021 at Aarhus University Hospital in Denmark. Tumor samples were obtained during transurethral resection of the bladder at the time of diagnosis (n = 112) and blood samples were collected at scheduled clinical visits. Patients without clinical recurrence had median follow-up of 1841 d after RC. All patients provided informed written consent, and the study was approved by The National Committee on Health Research Ethics (#1302183 and #1706291).

2.2. Whole-genome sequencing

Libraries of tumor and matching germline DNA were prepared using the Twist Library preparation EF kit (Twist Bio-

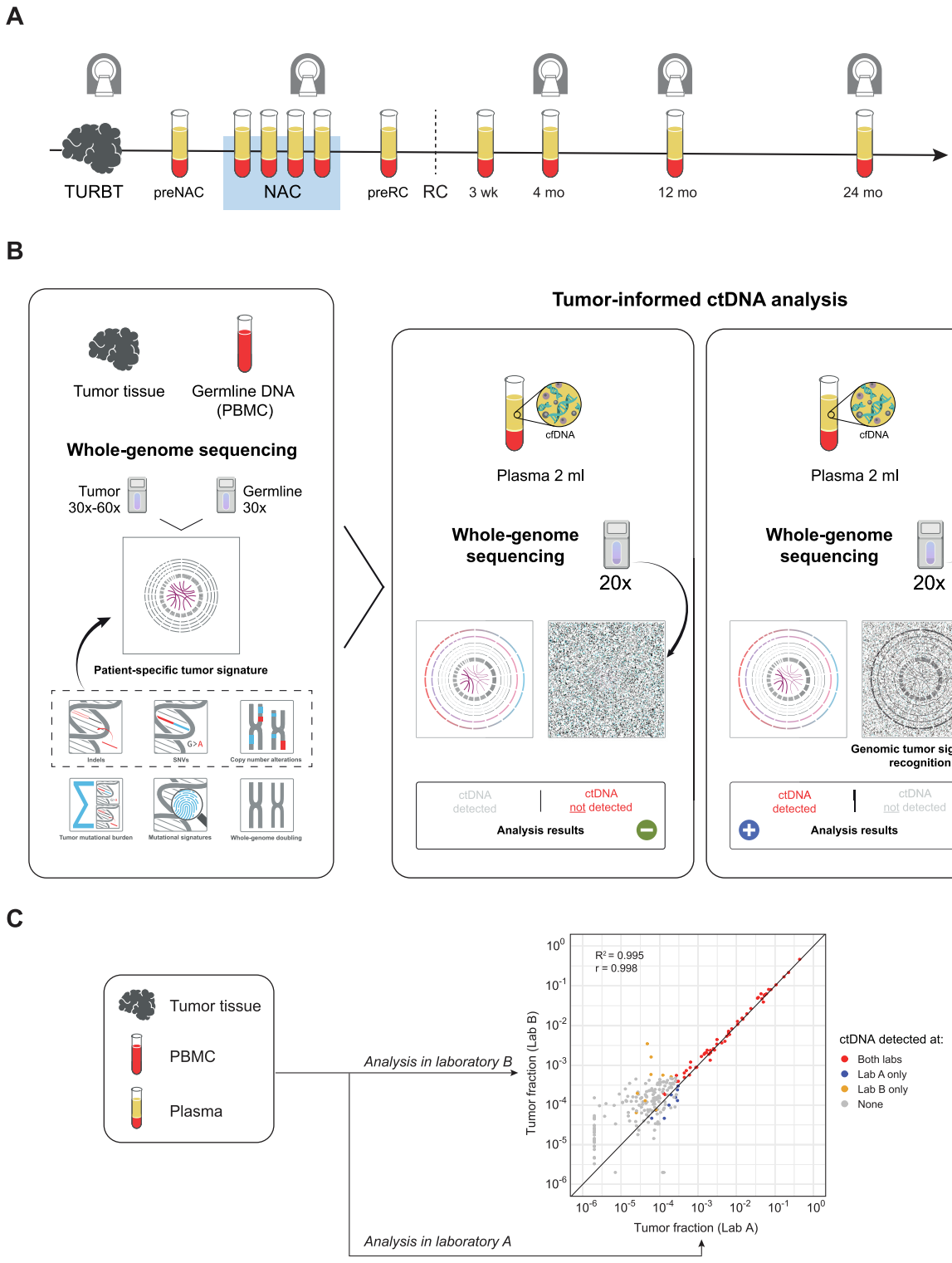

Fig. 1 – Study design and analysis scheme. (A) Study design showing the schedule for computed tomography (CT) scans (thorax-abdomen) and clinical sample collection. To exclude distant metastasis, full body positron emission tomography/CT scans were performed after diagnosis. (B) Whole-genome sequencing (WGS) approach for detection of circulating tumor DNA (ctDNA). WGS of tumor/germline pairs was performed and patient-specific genomic tumor signatures were generated using signals from genome-wide alterations coupled with advanced signal processing and error suppression (panel 1). The patient-specific tumor signatures were used to determine the presence or absence of ctDNA in WGS data from plasma cell-free DNA (panels 2 and 3). (C) Reproducibility of the WGS-based ctDNA detection method was established via independent processing and analysis of technical replicates (tumor, PBMC, and plasma DNA) at two different laboratories (in Denmark and the USA). The Pearson correlation coefficient and the coefficient of determination are shown in the plot. The diagonal indicates $x = y$. TURBT = transurethral resection of bladder tumor; NAC = neoadjuvant chemotherapy; RC = radical cystectomy; PBMC = peripheral blood mononuclear cell.

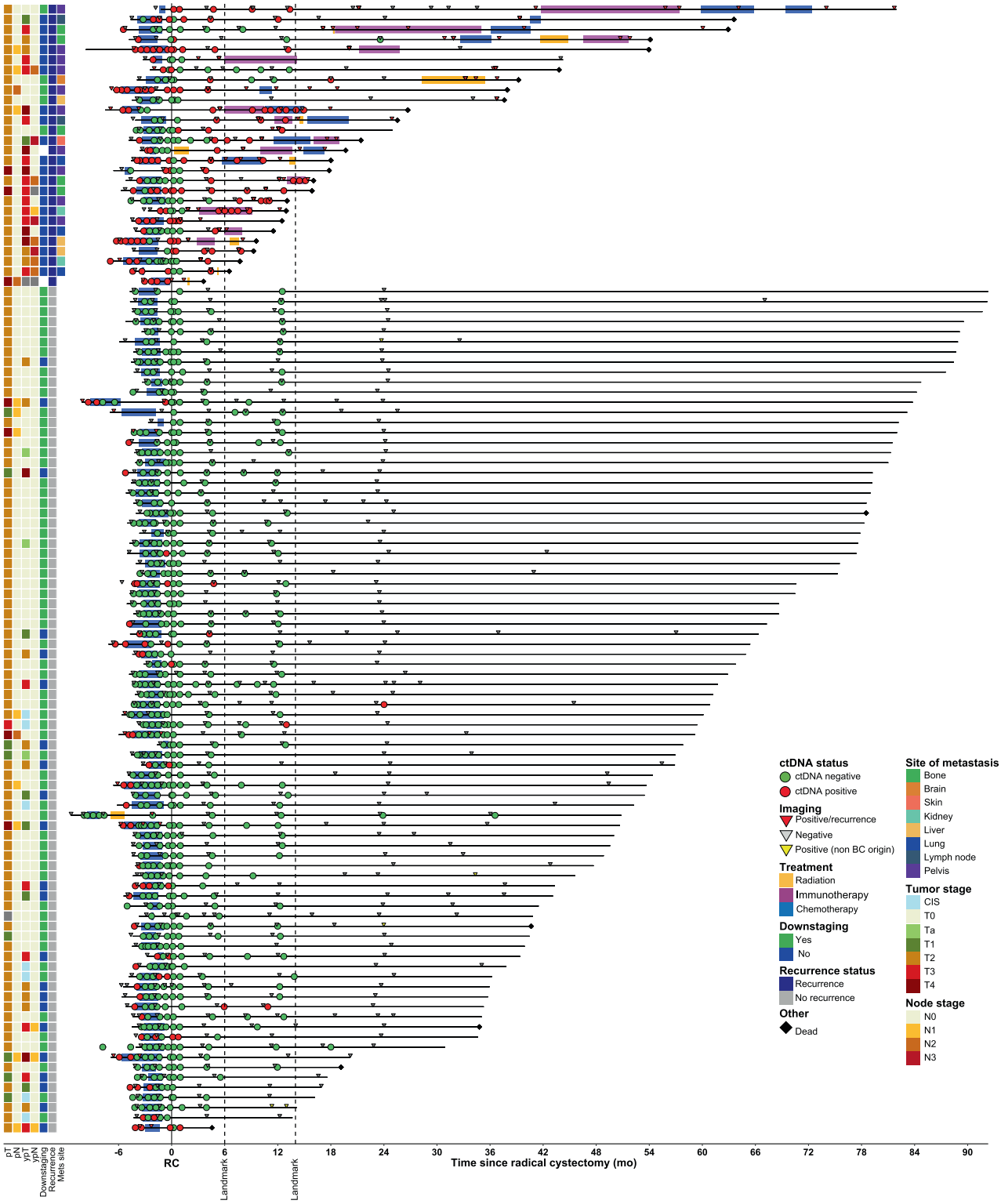

Fig. 2 – Longitudinal ctDNA results for all patients. Horizontal lines represent the disease course and circles denote ctDNA status. Treatment and imaging information is indicated for each patient as described in the color key. Patients are ordered by decreasing overall survival for patients with and without disease recurrence. Patients 4175 and 4250 were not able to undergo radical cystectomy; time 0 for these patients is the scheduled time for surgery. The 4-mo and 12-mo landmark lines are positioned at 6 mo and 14 mo, respectively, to encompass all delayed visits originally scheduled for the 4-mo and 12-mo time points. BC = bladder cancer; CIS = carcinoma in situ; ctDNA = circulating tumor DNA; IO = immuno-oncology agent; Mets = metastases.

science) with an input of 200 ng of DNA. Libraries of cell-free DNA (cfDNA) from plasma were prepared using a KAPA HyperPrep kit (Roche) with the xGEN UDI-UMI adapters (Integrated DNA Technologies) using a cfDNA input equal to 1–2 ml of plasma and seven cycles of polymerase chain reaction after ligation (minimum input of 5 ng). All libraries were paired-end sequenced (2 × 150 bp) on a NovaSeq 6000 platform (Illumina, San Diego, CA, USA).

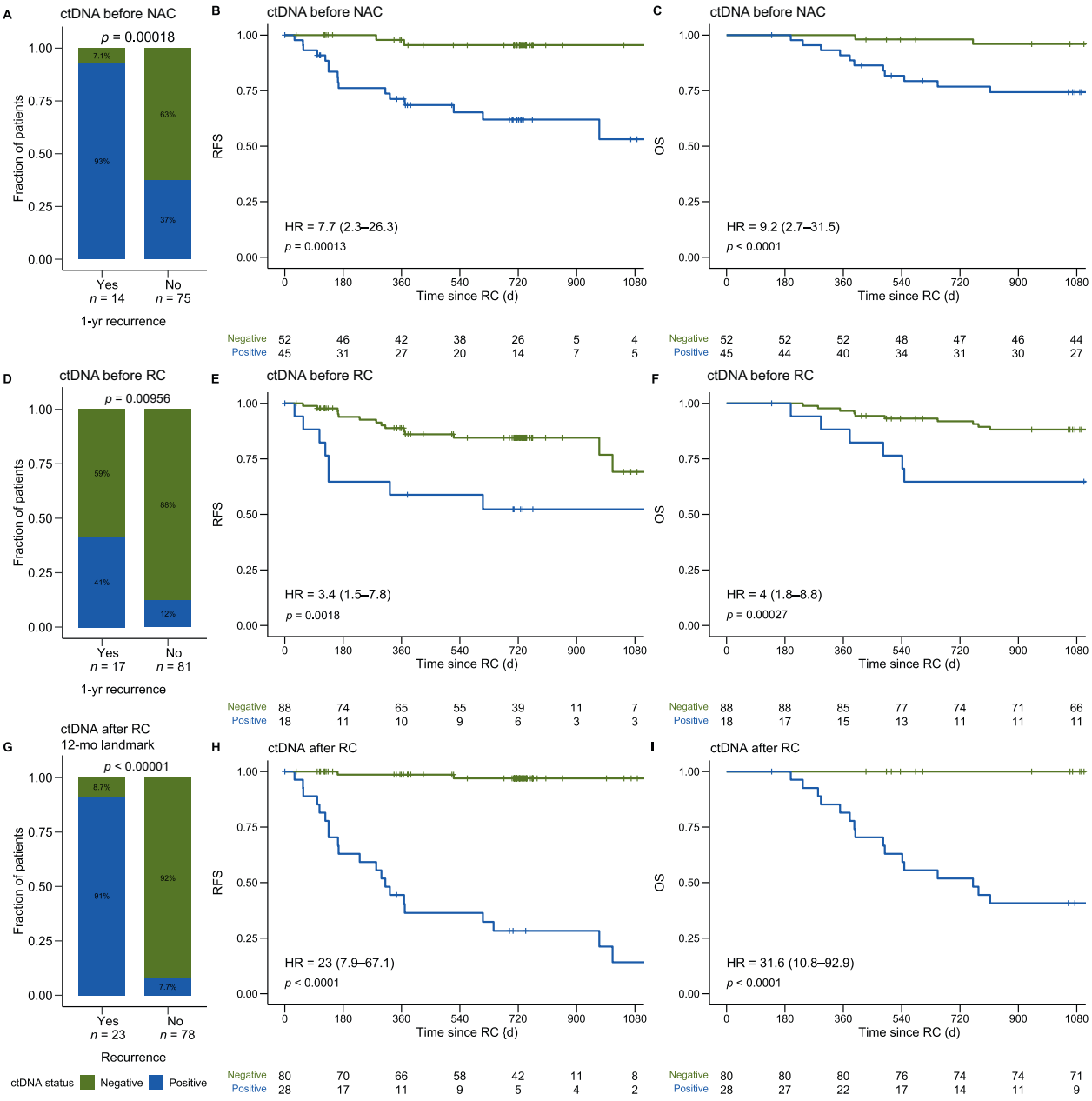

Fig. 3 – ctDNA detection for assessment of prognosis. (A) Association between plasma ctDNA status before NAC and recurrence status within 1 yr after RC. For patients without recurrence, only patients with at least 2 yr of follow-up after RC were included. (B, C) Kaplan-Meier analysis of (B) RFS and (C) OS by plasma ctDNA status before NAC. (D) Association between plasma ctDNA status before RC (after NAC) and recurrence status within 1 yr after RC. For patients without recurrence, only patients with at least 2 yr of follow-up after RC were included. (E, F) Kaplan-Meier analysis of (E) RFS and (F) OS by plasma ctDNA status before RC. (G) Association between accumulated plasma ctDNA status up until the 1-yr post-RC visit (12-mo landmark) and recurrence status within 18 mo after the last plasma sample was analyzed for ctDNA. For patients without recurrence, only patients with at least 18 mo of follow-up after the last plasma sample were included. (H, I) Kaplan-Meier analysis of (H) RFS and (I) OS by accumulated plasma ctDNA status after RC. Hazard ratios (HRs), 95% confidence intervals (CIs; Cox regression), and corresponding *p* values (log-rank test) are shown on each Kaplan-Meier plot. The statistical significance of associations between ctDNA status and recurrence was determined using Fisher's exact test. ctDNA = circulating tumor DNA; NAC = neoadjuvant chemotherapy; OS = overall survival; RC = radical cystectomy; RFS = recurrence-free survival.

2.3. Estimation of tumor fraction in solid tumor tissue and cfDNA

The tumor fraction for both solid tumor samples and plasma samples was determined using a proprietary bioinformatics pipeline that uses techniques previously outlined [9]. Tumor samples with an estimated tumor fraction of <10% were discarded because of insufficient tumor signals for reliable mutation identification. The qualified tumor samples combined with the matched normal samples were used to generate patient-specific tumor signatures comprising the broad spectrum of somatic mutations found in the patient's tumor, including single nucleotide variants (SNVs), insertions and deletions (indels), and copy number alterations (CNAs). To

compensate for WGS artifacts, the signatures were cleaned by filtering out the components found in at least three out of 45 cfDNA samples from healthy individuals. In addition, cfDNA read-level error suppression was applied to remove SNV-like artifacts on the basis of concordance between overlapping read-pair sequences, as outlined by Zviran et al [9]. The cfDNA tumor fractions were estimated as the number of patient-specific tumor signature components detected divided by the total number of reads.

2.4. Statistical analysis

Survival and cumulative incidence curves were compared using the Kaplan-Meier method (log-rank tests). Hazard ratios (HRs) and corresponding 95% confidence intervals (CIs) were calculated using Cox regression analysis (R packages *survminer* version 0.4.9 and *survival* version 3.2.13; R Foundation for Statistical Computing, Vienna, Austria). The Kruskal-Wallis test, Wilcoxon rank-sum test, Fisher's exact test, and Pearson's correlation coefficient were used to determine statistical significance of associations.

3. Results

3.1. Patient characteristics and WGS data generation

A total of 112 patients with localized MIBC treated with NAC before RC were prospectively enrolled for longitudinal ctDNA analysis at Aarhus University Hospital, Denmark (Fig. 1A and Supplementary Table 1). RC was performed for 110 of the patients, with median follow-up of 53.6 mo after RC. We observed a recurrence rate of 24% (26/110), pathologic downstaging to a noninvasive stage (≤ypTa/Tis N0) for 61% (67/110) of the patients, and a pathologic complete response (ypT0/Tis N0) for 58% (64/110). WGS of tumor and matched peripheral blood mononuclear cell (PBMC) DNA was performed at a mean genome coverage of 59× (range 35×–106×) for formalin-fixed, paraffin-embedded tissue, 33× (range 28×–127×) for fresh-frozen samples, and 31× (range 11×–108×) for PBMC DNA. WGS of cfDNA from plasma samples (n = 916) was performed at a mean genome coverage of 28× (range 20×–90×).

3.2. ctDNA detection via tumor-informed WGS models

For ctDNA detection we developed patient-specific, tumor-informed WGS models by integrating genome-wide somatic alteration patterns with advanced signal processing and error suppression (Fig. 1B). The patient-specific models were applied to WGS data for plasma cfDNA for ctDNA detection. For initial validation of the robustness of the WGS ctDNA analysis pipeline, we evaluated technical replicates (tumor, PBMC, and plasma DNA) analyzed independently in two different laboratories (USA and Denmark) using similar protocols. The ctDNA calls were concordant for 92% (208/226) of the plasma samples, and high correlation of estimated tumor fractions between laboratory sites was observed (R^2 = 0.995, r = 0.998; Fig. 1C). Site-specific protocol factors such as sequencing depth are a likely source of the variation in ctDNA calls for the remaining 8% (18/226) of samples, indicating a need for standardized sequencing strategies.

3.3. ctDNA analysis for assessment of prognosis and detection of recurrence

The prognostic value of ctDNA was investigated using 916 plasma samples collected during the disease courses for the 112 patients (Fig. 2 and Supplementary Fig. 1). Detection of ctDNA was highly prognostic of patient outcomes at diagnosis before NAC (recurrence-free survival [RFS]: HR 7.7, 95% CI 2.3–26.3; p = 0.0001; overall survival [OS]: HR 9.2, 95% CI 2.7–31.5; p = 0.0001), after NAC and before RC (RFS: HR 3.4, 95% CI 1.5–7.8; p = 0.0018; OS: HR 4, 95% CI 1.8–8.8; p = 0.0003), and during disease surveillance after RC (accumulated ctDNA status up to 1 yr after RC; RFS: HR 23, 95% CI 7.9–67.1; p < 0.0001; OS: HR 31.6, 95% CI 10.8–92.9; p < 0.0001. The results are shown in Figure 3 and Supplementary Table 2.

To evaluate post-RC ctDNA detection within a landmark analysis framework, we used the accumulated ctDNA status up to the 1-yr post-RC visit as the 12-mo landmark. The recurrence status of the patients was evaluated within an 18-mo period following the last ctDNA analysis. For patients without recurrence, only patients with at least 18 mo of follow-up after the last plasma sample were included. Landmark ctDNA positivity was observed for 27/101 patients evaluable for landmark MRD analysis (27%), of whom 21 had recurrence within 18 mo after the last ctDNA analysis (sensitivity 91% and specificity 92%; Fig. 3G). In addition, to increase clinical translatability for guiding adjuvant treatment, we evaluated the accumulated ctDNA status up to the 4-mo visit after RC. ctDNA analysis at the 4-mo landmark identified disease recurrence with sensitivity of 87% and specificity of 94% when using the same follow-up period as for the 12-mo landmark.

In 70% of patients with recurrence (18/26), ctDNA was detected before clinical recurrence on radiographic imaging (including full follow-up of the patients; Fig. 2). Overall, the median lead time with ctDNA detection was 131 d (range −106 to 1156; p < 0.00001) over radiographic imaging for patients with detectable ctDNA after RC (full follow-up; Fig. 4A). To assess the value of serial ctDNA monitoring, we calculated the cumulative incidence of ctDNA detection after RC (Fig. 4B). Among patients with recurrence, the cumulative ctDNA detection was 85% (22/26) at 1 yr after RC, in comparison to 6% for patients without recurrence (5/82; p < 0.0001). Notably, 95% (21/22) of all ctDNA-detected recurrences were found within the first 6 mo after RC (Fig. 4B).

As the level of ctDNA detected after RC varied, we hypothesized that the tumor fraction could be related to the metastatic site. Interestingly, we observed significantly lower tumor fractions for patients with lung metastasis in comparison to metastasis at other sites (Fig. 4C, D).

3.4. ctDNA monitoring for evaluation of treatment response

ctDNA status before NAC (p < 0.00001) and before RC (p = 0.009) was significantly associated with pathologic downstaging (Fig. 4E, F and Supplementary Fig. 2). ctDNA

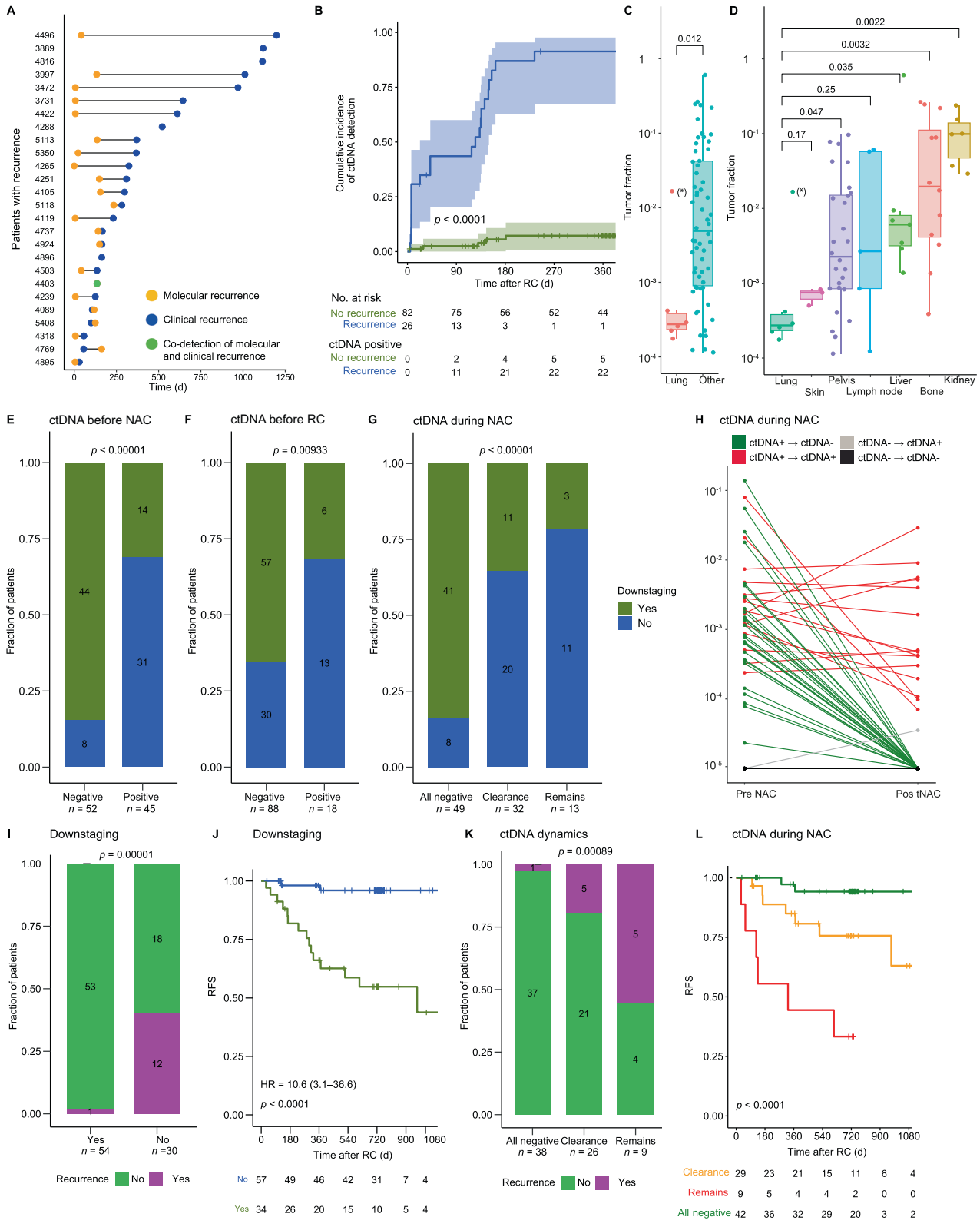

dynamics during NAC, that is, whether ctDNA remained detectable, remained undetectable, or was cleared, was also a predictor of pathologic downstaging ($p < 0.00001$; Fig. 4G, H). Pathologic downstaging was per se a strong predictor of recurrence, with a recurrence rate of 2% (one of 54) for patients with and 40% (12/30) for patients without pathologic downstaging (Fig. 4I, J). While pathologic downstaging uses the local tumor response to NAC as a proxy for systemic response, ctDNA status before RC provides a direct measure of metastatic disease burden. Patients remaining ctDNA-positive throughout NAC ($n = 9$) had particularly poor outcomes, while patients remaining ctDNA-negative during NAC ($n = 38$) had favorable outcomes, with only one patient experiencing recurrence within 1 yr after RC (Fig. 4K, L). For patients with ctDNA clearance during NAC, 19% (five of 26) experienced recurrence within 1 yr.

3.5. Genomic characterization of primary tumors

WGS analysis of the primary tumor for 112 patients revealed a median of 23 851 SNVs and 674 indels per tumor, which is comparable to a previous WGS analysis of bladder tumors [11]. *TP53*, *RB1*, *KMT2D*, *ARID1A*, and *KDM6A* were the genes most frequently mutated, and 55% of tumors had a *TERT* promoter mutation (Supplementary Fig. 3A and Supplementary Table 3). Whole-genome doubling (WGD) was identified in 51% of tumors (57/112; Supplementary Fig. 3B). WGD has been associated with worse prognosis [12]; however, we observed no correlation to worse RFS or OS (Supplementary Fig. 3C, D).

We performed de novo extraction of single-base substitution (SBS) signatures and small insertion-and-deletion (ID) signatures (Supplementary Fig. 3A). Among the SBS signatures extracted, APOBEC-induced mutagenesis was identified as the primary contributor to the mutational landscape of the tumors; the median percentage of SNVs per patient attributed to SBS2 or SBS13 mutational contexts was 42%. Among the ID signatures extracted, ID1, ID3, and ID8 were identified as the primary contributors, each accounting for >15% of all indels observed. We observed that tumors from current smokers had a significantly higher number of SBS92-related mutations in comparison to tumors from former and never smokers ($p < 0.0001$; Supplementary Fig. 4A), in line with previous studies linking SBS92 to smoking-induced mutagenesis in both malignant and nonmalignant bladder tissue [13,14]. Of note, patient 5350 had a novel SBS signature characterized by T → A and T → C mutations (referred to as SBSX; Supplementary Fig. 5) that could not be reconstructed using known signatures in existing databases [15,16]. The note in the Supplementary material provides details on SBSX and extended genomic characterization of tumors.

3.6. Tumor evolution according to WGS-based ctDNA analysis

WGS of cfDNA from plasma samples with a high tumor fraction allows characterization of genomic changes occurring de novo in ctDNA, that is, genomic changes not detected in the tumor biopsies [17,18]. Using plasma WGS data, we explored the potential for plasma-based characterization of tumor evolution using ~20× WGS. For 38% of the patients with recurrence (ten of 26), the cfDNA tumor fraction was sufficient (>10%) to perform de novo somatic variant calling independent of the initial tumor biopsy (performed for 15 plasma samples for those ten patients). Six plasma samples from four patients (5408, 5113, 4119, and 4105; 40% of the plasma samples included) showed a contribution of the platinum therapy–associated mutational signatures SBS31 and SBS35 (Fig. 5A). As expected, the two chemotherapy-induced mutational signatures were not observed in any of the primary tumors (collected before NAC) and were only observed for plasma-specific mutations. For all four patients, the SBS31/35 signatures were observed in plasma samples collected 239–571 d after initiation of NAC (plasma samples collected earlier in the disease course for the patients were not characterized because the tumor fraction was too low). None of the four patients had a pathologic response to NAC; however, the presence of chemotherapy-induced mutational signatures in the plasma samples may indicate clonal expansion after gemcitabine/cisplatin treatment.

We observed evolution of the CNAs detected in post-treatment plasma samples in comparison to the primary tumor for all ten patients, suggesting that the metastatic lesion differs from the sequenced part of the primary tumor (Fig. 5B and Supplementary Fig. 6). In the two plasma samples collected after RC for patient 4105 (one of the patients who had chemotherapy-induced mutational signatures), we observed a focal amplification on chromosome 4 affecting

Fig. 4 – ctDNA measurement for detection of recurrence and treatment response. (A) Lead time in days between molecular recurrence (ctDNA positivity) and clinical recurrence (positive radiographic imaging). The statistical significance of differences was calculated using a paired Wilcoxon signed-rank test. (B) Cumulative incidence of ctDNA detection after RC. (C) Association between the plasma-based tumor fraction and the metastatic site of the recurrence detected. Only post-RC samples with a tumor fraction above zero were included and more than one plasma sample per patient could be included in the analysis. The asterisk denotes an outlier observed in a patient with concurrent lung and brain metastases. (D) Association between the ctDNA tumor fraction and lung metastases versus other metastatic sites. Only post-RC samples with a tumor fraction above zero were included and more than one plasma sample per patient could be included in the analysis. The asterisk denotes an outlier observed in a patient with concurrent lung and brain metastases. (E, F) Association between ctDNA status (E) before NAC and (F) before RC and downstaging. (G) Association between ctDNA clearance after NAC and pathological downstaging. (H) Comparison of ctDNA tumor fractions before and after NAC. Colors indicate whether ctDNA remained detectable (red), remained undetectable (black), was cleared during NAC (green), or appeared (gray). (I) Association between pathological downstaging and recurrence status within 1 yr after RC for patients who received at least three cycles of NAC. (J) Kaplan-Meier analysis of RFS by pathological downstaging status for patients who received at least three cycles of NAC. (K) Association between ctDNA clearance after NAC and recurrence status within 1 yr after RC for patients who received at least three cycles of NAC. (L) Kaplan-Meier analysis of RFS by ctDNA clearance status after NAC for patients who received at least three cycles of NAC. ctDNA = circulating tumor DNA; NAC = neoadjuvant chemotherapy; OS = overall survival; RC = radical cystectomy; RFS = recurrence-free survival.

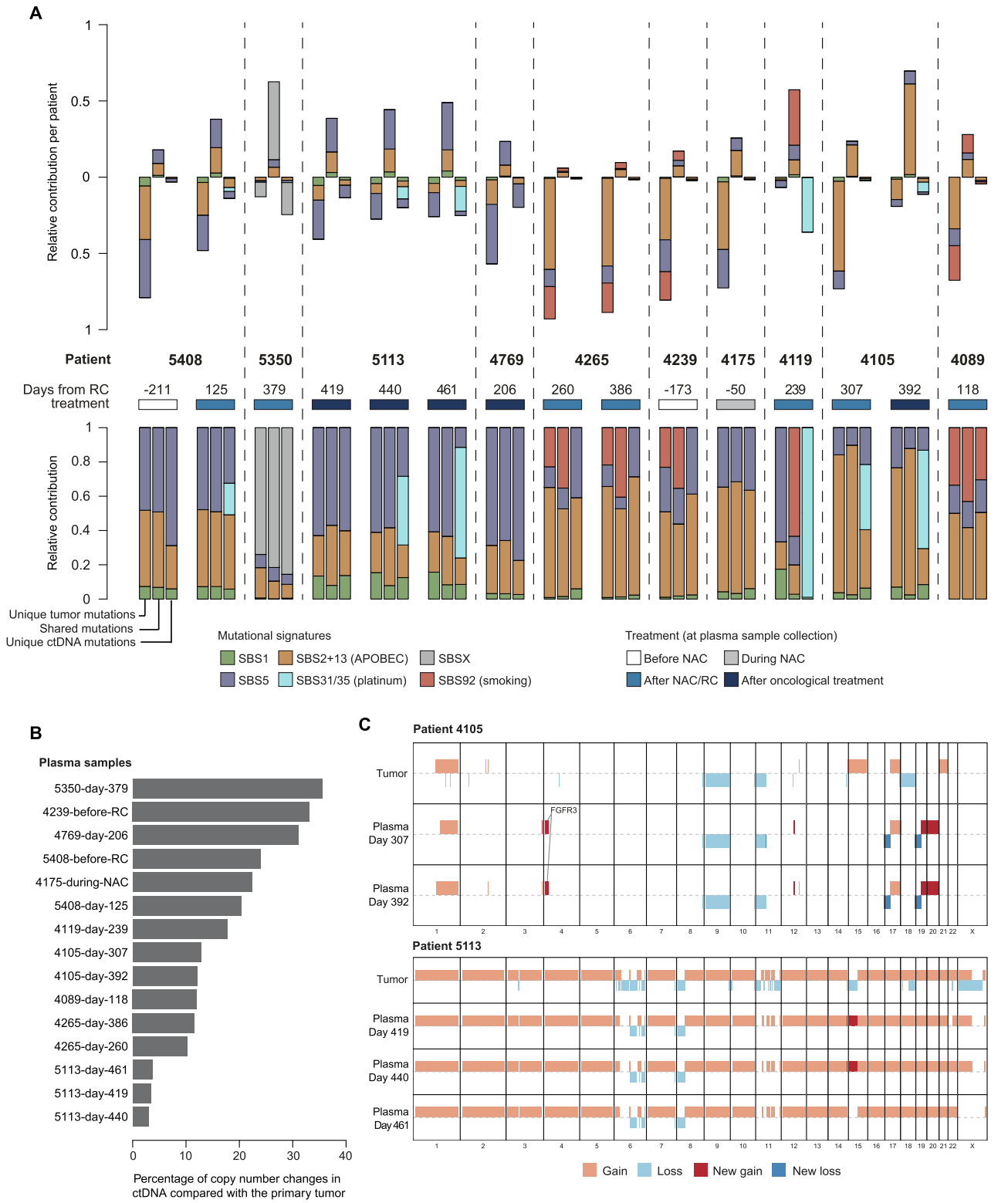

Fig. 5 – Genomic characterization of plasma samples with a high tumor fraction. (A) Relative contribution of mutational signatures in primary tumors and plasma samples with a tumor fraction >10%. Each patient is represented by three bars corresponding to the contribution of signatures for mutations present only in the primary tumor (left), mutations present both in the primary tumor and ctDNA (middle), and mutations present exclusively in ctDNA (right). The top panel indicates the fraction of mutations that are shared or unique to either tumor or plasma for each patient, whereas the lower panel is normalized by the total number of SNVs per sample. The day for plasma sample collection in relation to RC is shown along with the treatment status at sample collection. (B) The percentage of genome-wide copy number changes in ctDNA in comparison to the initial primary tumor sample for all plasma samples with a tumor fraction >10%. (C) Examples of changes in copy numbers between the primary tumor (top row) and ctDNA (following rows) for patient 4105 and 5113. ctDNA = circulating tumor DNA; NAC = neoadjuvant chemotherapy; RC = radical cystectomy.

the primary tumor driver variant *FGFR3* p.S249C, and an increase in copy number on chromosomes 19q and 20 not detected in the primary tumor (Fig. 5C). In the plasma sample collected during NAC for patient 5408, newly acquired copy-number gains on chromosomes 17, 19p, and 22 were observed (Supplementary Fig. 6). In contrast to these large genomic changes, the three plasma samples collected after RC for patient 5113 were all highly representative of the primary tumor, with only few recurrence-acquired variations, indicating limited evolution after treatment (Fig. 5C).

4. Discussion

We used a WGS approach to monitor ctDNA in patients with localized MIBC and documented the prognostic role of ctDNA at diagnosis, before RC, and during surveillance. Our findings underline a role for ctDNA in guiding treatment decisions in bladder cancer, in line with previous findings for other patient cohorts [3,4,6,19,20]. An important aspect of the WGS approach is its high sensitivity and specificity, which are comparable to other established tumor-informed ctDNA tests applied in this setting, matched with the ease of performing WGS without any need for the design of personalized assays. WGS-based ctDNA analysis facilitates local sample processing and rapid generation of test results, and may thus drive the ctDNA field forwards faster and pave the way for novel trial designs requiring immediate test results. Prospective WGS-based ctDNA analysis for MRD detection seems very promising with low false-negative rates, and may soon be implemented for informed selection of patients for adjuvant treatments. In line with this, ongoing clinical trials will demonstrate if early ctDNA-guided treatment in the adjuvant setting is more beneficial in comparison to treatment initiation on detection of recurrence via radiographic imaging [21,22]. In addition, our study supports the rationale behind investigating the benefit of NAC administration for ctDNA-negative patients and whether bladder-sparing approaches can be applied on the basis of ctDNA testing.

We identified significantly lower tumor fractions for patients with lung metastasis in comparison to metastasis at other sites, indicating a correlation between the extent of detectable ctDNA and the location of metastasis. These findings are in accordance with a recent study on metastatic colorectal cancer that showed that patients with lung-only and peritoneum-only metastatic disease had significantly lower levels of ctDNA in comparison to patients with metastasis at other sites [23], indicating a lower detection sensitivity. WGS-based ctDNA detection approaches may potentially result in better MRD detection in patients with lung metastasis.

Our WGS strategy for ctDNA detection allows direct genomic characterization of plasma cfDNA independently of the initial tumor biopsy. With a greater sequencing depth and accompanying deep targeted sequencing of the variants detected, this approach holds potential for increasing our understanding of tumor evolution and treatment resistance mechanisms. It has been demonstrated that ctDNA contains multiple subclones and that synchronous metastatic tissue biopsies only comprise a small fraction of the total ctDNA [24]. Analysis of plasma samples can thereby overcome tissue sampling bias leading to clonal illusion and underestimated heterogeneity to recapitulate complete metastatic tumor biology [25]. Furthermore, tumor evolution and therapy-induced shifts in selection pressure can be longitudinally tracked. In the post-treatment plasma samples for patient 4105, we observed an acquired focal amplification of the *FGFR3* gene on chromosome 4, indicating that erdafitinib (pan-FGFR inhibitor) could be a potential treatment option for this patient. This observation highlights the importance of having a real-time snapshot of the current tumor biology when making treatment decisions in the metastatic setting to improve identification of therapeutic targets and provide information on possible treatment resistance at an early time point. Among the patients with recurrence (n = 26, full follow-up included), only four had negative ctDNA status after RC. Future studies investigating non–tumor-informed genomic characterization of post-treatment plasma samples may be relevant for identification of novel genomic alterations acquired during tumor evolution. This may demonstrate that the tumor-informed ctDNA detection was limited by the tumor biopsy analyzed and/or extensive tumor evolution.

The sequencing depth of ~28× is a limitation for assessing individual sites; a greater sequencing depth is required to improve the genomic characterization and study clinically actionable gene mutations. A greater sequencing depth might also allow biological characterization of plasma samples with a tumor fraction below the currently applied cutoff of 10%. Furthermore, to build on our findings presented here, WGS of metastatic tissue biopsies could be performed to study whether ctDNA profiling provides a more complete genomic characterization of all metastatic tumor sites in comparison to analysis of a single metastatic lesion, as has previously been demonstrated in advanced prostate cancer [24].

5. Conclusions

Our study shows that WGS-based analysis of cfDNA allows ultrasensitive ctDNA detection in patients with MIBC. ctDNA testing holds huge potential to change the current clinical management of patients towards more individualized treatment. We also showed that the WGS-based ctDNA detection approach provides an opportunity to perform de novo characterization of genomic changes acquired after treatment, which is not possible with bespoke ctDNA detection methods. Plasma-based tracking of tumor evolution may ultimately open opportunities to refine precision oncology.

Author contributions: Lars Dyrskjøt had full access to all the data in the study and takes responsibility for the integrity of the data and the accuracy of the data analysis.

Study concept and design: Nordentoft, Zviran, Oklander, Dyrskjøt.
Acquisition of data: Nordentoft, Birkenkamp-Demtröder, Frydendahl, Dyrskjøt.
Analysis and interpretation of data: Nordentoft, Lindskrog, Birkenkamp-Demtröder, Gonzalez, Polak, Afterman, Lamy, Knudsen, Dyrskjøt.
Drafting of the manuscript: Nordentoft, Lindskrog, Dyrskjøt.

Critical revision of the manuscript for important intellectual content: All authors.
Statistical analysis: Nordentoft, Lindskrog, Gonzalez.
Obtaining funding: Dyrskjøt.
Administrative, technical, or material support: Jensen, Dyrskjøt.
Supervision: Dyrskjøt.
Other: None.

Financial disclosures: Lars Dyrskjøt certifies that all conflicts of interest, including specific financial interests and relationships and affiliations relevant to the subject matter or materials discussed in the manuscript (eg, employment/affiliation, grants or funding, consultancies, honoraria, stock ownership or options, expert testimony, royalties, or patents filed, received, or pending), are the following: Lars Dyrskjøt has sponsored research agreements with C2i Genomics, Natera, AstraZeneca, Photocure, and Ferring; has an advisory/consulting role for Ferring, MSD, and UroGen; has received speaker honoraria from AstraZeneca, Pfizer, and Roche; has received travel support from MSD; and is a board member for BioXpedia. Jørgen Bjerggaard Jensen is an advisory board member for Ferring, Roche, Cepheid, Urotech, Olympus, AMBU, Janssen, and Cystotech; is a speaker for medac, Olympus, Intuitive Surgery, and Photocure ASA; and has research collaborations with medac, Photocure ASA, Roche, Ferring, Olympus, Intuitive Surgery, Astellas, Cepheid, Nucleix, Urotech, Pfizer, AstraZeneca, MeqNordic, Laborie, VingMed, AMBU, and Cystotech. Asaf Zviran is the co-founder of C2i Genomics. Boris Oklander is the co-founder and chief technical officer of C2i Genomics. Santiago Gonzalez, Maja Kuzman, Jurica Levatic, Dunja Glavas, Ryan Ptashkin, James Smadbeck, Danielle Afterman, Tomer Lauterman, Yarin Cohen, Zohar Donenhirsh, Iman Tavassoly, and Ury Alon are employees of C2i Genomics. Paz Polak is a former employee of C2i Genomics. The remaining authors have nothing to disclose.

Funding/Support and role of the sponsor: This work was funded by research grants to Lars Dyrskjøt from C2i Genomics, The Danish Cancer Society, Novo Nordisk Foundation, Independent Research Fund Denmark, Aarhus University, and Aarhus University Hospital. The sponsors played a role in the design and conduct of the study, management and analysis of the data, and approval of the manuscript.

Acknowledgments: We would like to thank technical personnel at the Departments of Molecular Medicine, Urology, and Oncology at Aarhus University Hospital for sample handling and processing. Sample collection was supported by the Danish Cancer Biobank.

Data sharing statement: The raw sequencing data generated in this study are not publicly available as this compromises patient consent and ethics regulations in Denmark. Processed nonsensitive data are available on request from the corresponding author.

Supplementary data

Supplementary data to this article can be found online at https://doi.org/10.1016/j.eururo.2024.05.014.

References

[1] Reinert T, Henriksen TV, Christensen E, et al. Analysis of plasma cell-free DNA by ultradeep sequencing in patients with stages I to III colorectal cancer. JAMA Oncol 2019;5:1124–31. https://doi.org/10.1001/jamaoncol.2019.0528.
[2] Abbosh C, Birkbak NJ, Wilson GA, et al. Phylogenetic ctDNA analysis depicts early-stage lung cancer evolution. Nature 2017;545:446–51.
[3] Christensen E, Birkenkamp-Demtröder K, Sethi H, et al. Early detection of metastatic relapse and monitoring of therapeutic efficacy by ultra-deep sequencing of plasma cell-free DNA in patients with urothelial bladder carcinoma. J Clin Oncol 2019;37:1547–57.
[4] Powles T, Assaf ZJ, Davarpanah N, et al. ctDNA guiding adjuvant immunotherapy in urothelial carcinoma. Nature 2021;595:432–7.
[5] Szabados B, Kockx M, Assaf ZJ, et al. Final results of neoadjuvant atezolizumab in cisplatin-ineligible patients with muscle-invasive urothelial cancer of the bladder. Eur Urol 2022;82:212–22.
[6] van Dorp J, Pipinikas C, Suelmann BBM, et al. High- or low-dose preoperative ipilimumab plus nivolumab in stage III urothelial cancer: the phase 1B NABUCCO trial. Nat Med 2023;29:588–92. https://doi.org/10.1038/s41591-022-02199-y.
[7] Witjes JA, Bruins HM, Cathomas R, et al. European Association of Urology guidelines on muscle-invasive and metastatic bladder cancer: summary of the 2020 guidelines. Eur Urol 2021;79:82–104.
[8] Moser T, Kühberger S, Lazzeri I, Vlachos G, Heitzer E. Bridging biological cfDNA features and machine learning approaches. Trends Genet 2023;39:285–307. https://doi.org/10.1016/j.tig.2023.01.004.
[9] Zviran A, Schulman RC, Shah M, et al. Genome-wide cell-free DNA mutational integration enables ultra-sensitive cancer monitoring. Nat Med 2020;26:1114–24.
[10] Widman AJ, Shah M, Øgaard N, et al. Machine learning guided signal enrichment for ultrasensitive plasma tumor burden monitoring. bioRxiv preprint. https://doi.org/10.1101/2022.01.17.476508.
[11] ICGC/TCGA Pan-Cancer Analysis of Whole Genomes Consortium. Pan-cancer analysis of whole genomes. Nature 2020;578:82–93.
[12] Bielski CM, Zehir A, Penson AV, et al. Genome doubling shapes the evolution and prognosis of advanced cancers. Nat Genet 2018;50:1189–95.
[13] Lawson ARJ, Abascal F, Coorens THH, et al. Extensive heterogeneity in somatic mutation and selection in the human bladder. Science 2020;370:75–82.
[14] Islam SMA, Díaz-Gay M, Wu Y, et al. Uncovering novel mutational signatures by de novo extraction with SigProfilerExtractor. Cell Genom 2022;2:100179.
[15] Tate JG, Bamford S, Jubb HC, et al. COSMIC: the Catalogue Of Somatic Mutations In Cancer. Nucleic Acids Res 2019;47:D941–7.
[16] Degasperi A, Amarante TD, Czarnecki J, et al. A practical framework and online tool for mutational signature analyses show inter-tissue variation and driver dependencies. Nat Cancer 2020;1:249–63.
[17] Adalsteinsson VA, Ha G, Freeman SS, et al. Scalable whole-exome sequencing of cell-free DNA reveals high concordance with metastatic tumors. Nat Commun 2017;8:1324.
[18] Parikh AR, Leshchiner I, Elagina L, et al. Liquid versus tissue biopsy for detecting acquired resistance and tumor heterogeneity in gastrointestinal cancers. Nat Med 2019;25:1415–21.
[19] Patel KM, van der Vos KE, Smith CG, et al. Association of plasma and urinary mutant DNA with clinical outcomes in muscle invasive bladder cancer. Sci Rep 2017;7:5554.
[20] Vandekerkhove G, Lavoie JM, Annala M, et al. Plasma ctDNA is a tumor tissue surrogate and enables clinical-genomic stratification of metastatic bladder cancer. Nat Commun 2021;12:184.
[21] Bjerggaard Jensen J. Treatment of metastatic bladder cancer at the time of biochemical relapse following radical cystectomy. https://clinicaltrials.gov/ct2/show/NCT04138628.
[22] Hoffmann-La Roche. A study of atezolizumab versus placebo as adjuvant therapy in patients with high-risk muscle-invasive bladder cancer who are ctDNA positive following cystectomy. https://clinicaltrials.gov/ct2/show/NCT04660344.
[23] Bando H, Nakamura Y, Taniguchi H, et al. Effects of metastatic sites on circulating tumor DNA in patients with metastatic colorectal cancer. JCO Precis Oncol 2022;6:e2100535.
[24] Herberts C, Annala M, Sipola J, et al. Deep whole-genome ctDNA chronology of treatment-resistant prostate cancer. Nature 2022;608:199–208.
[25] Abbosh C, Frankell AM, Harrison T, et al. Tracking early lung cancer metastatic dissemination in TRACERx using ctDNA. Nature 2023;616:553–62.